Hepatocyte-specific c-Met Deletion Disrupts Redox Homeostasis and Sensitizes to Fas-mediated Apoptosis*

Luis E. Gómez-Quiroz, Valentina M. Factor, Pal Kaposi-Novak, Cedric Coulouarn, Elizabeth A. Conner, and Snorri S. Thorgeirsson[1]

From the Laboratory of Experimental Carcinogenesis, Center for Cancer Research, NCI, National Institutes of Health, Bethesda, Maryland 20892

The hepatocyte growth factor and its receptor c-Met direct a pleiotropic signal transduction pathway that controls cell survival. We previously demonstrated that mice lacking c-Met (Met-KO) in hepatocytes were hypersensitive to Fas-induced liver injury. In this study, we used primary hepatocytes isolated from Met-KO and control (Cre-Ctrl) mice to address more directly the protective effects of c-Met signaling. Loss of c-Met function increased sensitivity to Fas-mediated apoptosis. Hepatocyte growth factor suppressed apoptosis in Cre-Ctrl but not Met-KO hepatocytes concurrently with up-regulation of NF-κB and major antiapoptotic proteins Bcl-2 and Bcl-xL. Intriguingly, Met-KO hepatocytes exhibited intrinsic activation of NF-κB as well as Bcl-2 and Bcl-xL. Furthermore, unchallenged Met-KO cells displayed oxidative stress as evidenced by overproduction of reactive oxygen species, which was associated with greater NADPH and Rac1 activities, was blocked by the known NADPH oxidase inhibitors, and was paralleled by increased lipid peroxidation and reduced glutathione (GSH) content. *N*-Acetylcysteine, an antioxidant and GSH precursor, significantly reduced Jo2-induced cell death. Conversely, the GSH-depleting agent buthionine sulfoximine completely abolished the protective effects of *N*-acetylcysteine in Met-KO hepatocytes. In conclusion, genetic inactivation of c-Met in mouse hepatocytes caused defects in redox regulation, which may account for the increased sensitivity to Fas-induced apoptosis and adaptive up-regulation of NF-κB survival signaling. These data provide evidence that intact c-Met signaling is a critical factor in the protection against excessive generation of endogenous reactive oxygen species.

Fas (also known as APO-1/CD95) is a member of the death receptor family that signals via formation of a multiprotein complex termed death-inducing signaling complex followed by activation of downstream caspases (1). Fas is highly expressed in the liver, and it has been shown to rapidly activate apoptotic program leading to massive hepatocyte death when stimulated with agonistic anti-Fas (Jo2) antibody (2).

Hepatocyte growth factor (HGF)[2] is a ubiquitous and multifunctional cytokine that was originally identified as a potent mitogen for hepatocytes. All biological effects of HGF are mediated by a single tyrosine kinase receptor c-Met through concomitant activation of multiple intercellular effectors (3, 4). The signaling through the HGF/c-Met pathway regulates numerous cellular activities that vary depending on the cellular context (3, 5). There is strong genetic evidence that HGF/c-Met signaling is essential for hepatocyte survival. Targeted disruption of HGF or Met gene caused embryonic lethality because of multiple developmental defects, including massive apoptosis of fetal hepatocytes (6, 7).

A variety of studies shows that the levels of oxidative stress generated upon Fas stimulation play a prominent role in Fas-mediated apoptosis (8). Consequently, exposure to agents that increase cellular antioxidant defense or decrease the amount of reactive oxygen species (ROS) was able to interrupt the signaling cascade and prevent hepatocyte apoptosis induced by Fas agonist (9).

Accumulating data suggest that HGF may function as an antioxidant factor able to protect against oxidative stress-mediated cell killing through modulation of intracellular levels of GSH, a major determinant of cellular redox potential, and cytoprotective enzymes (10, 11). Furthermore, c-Met-triggered phosphoinositide 3-kinase(PI3K)/Akt activation, a key regulator of cell survival in adult and developing livers (12–14), has been shown to be involved in the control of intracellular oxidative stress (15). The PI3K/Akt signaling leads to the activation of the redox-sensitive transcription factor nuclear factor-κB (NF-κB), which in turn regulates expression of antioxidant and antiapoptotic target genes (16, 17). Consistent with this, we have recently demonstrated that c-Met-deficient hepatocytes display increased basal expression of a distinct set of genes implicated in the ROS defense system thus connecting c-Met to control of ROS metabolism (18, 19).

We previously demonstrated that mice lacking the c-Met receptor were hypersensitive to Fas-induced liver injury and died from fulminant hepatic failure after treatment with doses

---

[1] To whom correspondence should be addressed: 37 Convent Dr., Bldg. 37, Rm. 4146A, Bethesda, MD 20892-4262. Fax: 301-496-0734; E-mail: snorri_s_thorgeirsson@nih.gov.

[2] The abbreviations used are: HGF, hepatocyte growth factor; BSO, buthionine sulfoximine; DCFH-AM, diacetate, di(acetoxymethyl ester); DPI, diphenylene iodonium; Jo2, anti-mouse Fas monoclonal antibody; NAC, *N*-acetylcysteine; NaF, sodium fluoride; NF-κB, factor nuclear factor κB; PI3K, phosphoinositol 3-kinase; PI, propidium iodine; PMSF, phenylmethylsulfonyl fluoride; ROS, reactive oxygen species; MAPK, mitogen-activated protein kinase; HPLC, high pressure liquid chromatography; PKC, protein kinase C.

of anti-Fas antibody that did not affect the survival of wild-type mice (20). This study was undertaken to further characterize c-Met-triggered signaling pathways that regulate protection against Fas-induced apoptosis by using primary hepatocyte cultures established from liver-specific c-Met conditional knockout mice. The data show that c-Met inactivation sensitizes hepatocytes to Fas-mediated apoptosis via mechanisms involving increased NADPH-dependent ROS generation and GSH depletion.

EXPERIMENTAL PROCEDURES

Materials—Collagenase type I was obtained from Worthington). 6-Carboxy-2′,7′-dichlorodihydrofluorescein diacetate, di(acetoxymethyl ester) (DCFH-AM), and Hoechst 33342 were from Molecular Probes (Eugene, OR). Anti-mouse Fas monoclonal antibody (Jo2) was from Pharmingen. Recombinant human HGF was from PeproTech (Rocky Hill, NJ). STAT3 inhibitor peptide, wortmannin, LY294002, SN50, and PD98059 were from Calbiochem. All others chemicals were purchased from Sigma.

Mice, Hepatocyte Isolation, and Culture—c-met$^{fl/fl}$, Alb-Cre$^{+/-}$ (Met-KO), and control (w/w, AlbCre$^{+/-}$) (Cre-Ctrl) mice were described previously (20). Mice were maintained in pathogen-free housing and cared for in accordance with the NIH Guide for the Care and Use of Laboratory Animals. Hepatocytes were isolated from 8- to 10-week-old male mice by a two-step collagenase perfusion technique followed by isodensity purification in a Percoll gradient, as described previously (21), and were >90% viable as assessed by trypan blue exclusion. Hepatocytes were seeded at 5.3×10^4 cells per cm^2 either in Lab-Tek chambered slides or 10-cm dishes (Nalge, Nunc) in the Ham's F-12/Dulbecco's modified Eagle's basal hepatocyte growth medium supplemented with 10% fetal bovine serum (21). After a 4-h attachment, the medium was replaced to a serum-free basal hepatocyte growth medium. The following day, cells were exposed to Jo2 antibody (0.5 μg/ml) for 6 h, and as specified cells were pretreated with 40 ng/ml recombinant human HGF (PeproTech, Rocky Hill, NJ) or with various inhibitors of PI3K/Akt and NF-κB signaling, including wortmannin, PD98059, LY294002, SN50, sulfasalazine, and STAT3 inhibitor peptide at indicated concentrations.

Measurement of Apoptosis—Apoptotic cells were analyzed by staining with propidium iodine (PI) after fixation in methanol/acetic acid (3:1) as described previously (22). Apoptotic cells with characteristic nuclear fragmentation were counted in randomly chosen fields from two duplicate cultures. At least 500 cells were counted, and the frequency of apoptosis (apoptotic index) was expressed as a percentage of the total cell counted.

Analysis of Cellular Viability—Cell viability was assessed by the crystal violet-staining assay according to Nakagawa *et al.* (23). Cells seeded at 1×10^5 into 12-well plates were treated with 30 μM SN50 for 0, 6, 12, and 24 h, washed with PBS, fixed with 3.7% formaldehyde, and stained with 0.2% crystal violet. The absorbance of the 2% SDS extracts was measured at 620 nm. The cell viability was calculated as the percentage relative to untreated cells.

Western Blot Analysis—Total and nuclear proteins were isolated from cultured cells with T-PER or NE-PER (Pierce) extraction reagents, respectively, containing 1% Halt Protease Inhibitor Mixture (Pierce), 100 mM sodium fluoride, 1 mM phenylmethylsulfonyl fluoride (PMSF), and 50 mM sodium orthovanadate according to the manufacturer's protocols. One hundred μg of total protein or 25 μg of nuclear protein measured using BCA protein assay kit (Pierce) were separated on SDS-polyacrylamide gels (Invitrogen), transferred to polyvinylidene difluoride membranes (Invitrogen), and probed with anti-caspase 3, anti-Bcl-2, anti-Bcl-X$_L$, anti-Mcl-1, anti-cytochrome *c*, anti-IκB-α, anti-gp91^{Phox} (anti-Nox2) (Santa Cruz Biotechnology, Santa Cruz, CA), anti-cleaved caspase 3 (Trevigen, Gaithersburg, MD), anti-ERK1/2, anti-pERK1/2, anti-Akt, anti-pAkt, anti-PKC α/β II (Thr-638/641), anti-pPKC ζ/λ (Thr-410/403), anti-pPKC ϵ (Ser-729), anti-STAT3, and anti-pSTAT3 (Cell Signaling, Beverly, MA) antibodies. Membranes were incubated with anti-mouse or anti-rabbit horseradish peroxidase-conjugated secondary antibody depending on the origin of the primary antibody. Immunoreactive bands were identified with ECL-Plus Western blotting detection reagents (GE Healthcare). Equal loading was demonstrated by probing the same membranes with actin antibody (NeoMarker, Fremont, CA).

Electrophoretic Mobility Shift Assay—Nuclear extracts were prepared with Igepal CA-630 (0.58%) in 10 mM Hepes, pH 7.9, containing 10 mM KCl, 0.1 mM EDTA, 0.1 mM EGTA, 1 mM dithiothreitol, and 0.5 mM PMSF. Pelleted nuclei were resuspended in 20 mM Hepes, pH 7.9, containing 0.4 mM NaCl, 1 mM EDTA, 1 mM EGTA, 1 mM dithiothreitol, 1 mM PMSF. After mixing for 15 min at 4 °C, samples were centrifuged at 13,000 $\times$ *g* for 5 min, and the supernatant was recovered and stored at -80 °C. The protein concentration was determined by bovine serum albumin assay. NF-κB DNA binding activity was assayed using a consensus oligonucleotide 5′-AGTTGAGGGGACTT-TCCCAGGC-3′ (Promega, Madison, WI) as a probe. Probe was labeled with T4 polynucleotide kinase (U. S. Biochemical Corp.) and [γ-^{32}P]ATP (3000 Ci/mmol, MP Biomedical, Irving, CA) and purified using Bio-Spin 30 chromatography columns (Bio-Rad). The reaction mixture contained nuclear protein extract (20 μg) in 5 μl of incubation buffer (50 mM Tris-HCl, pH 7.5, 200 mM NaCl, 5 mM EDTA, 5 mM β-mercaptoethanol, 20% glycerol, 1 μg of dI-dC and ^{32}P-labeled probe. The reactions were electrophoresed on 6% polyacrylamide native gels. In competition experiments, 100-fold molar excess of nonlabeled oligonucleotide was included in the reaction mixture 5 min before addition of the labeled probe. For supershift analysis, nuclear extracts were incubated with 20 μg/ml anti-p65 (Santa Cruz Biotechnology) at room temperature for 15 min before addition of the labeled probe.

Analysis of Cellular ROS Levels by Confocal Microscopy—Reactive oxygen species (ROS) levels were determined using the redox-sensitive dye DCFH-DA. Cells seeded at 2.13×10^5 cells/cm^2 in Lab-Tek chambered cover glass were treated with 3 μM DCFH-AM for 30 min after overnight incubation in serum-free medium. Cells were washed two times with PBS, and the confocal images were acquired using a Zeiss LSM 510 NLO confocal microscope (Carl Zeiss, Inc., Thornwood, NY).
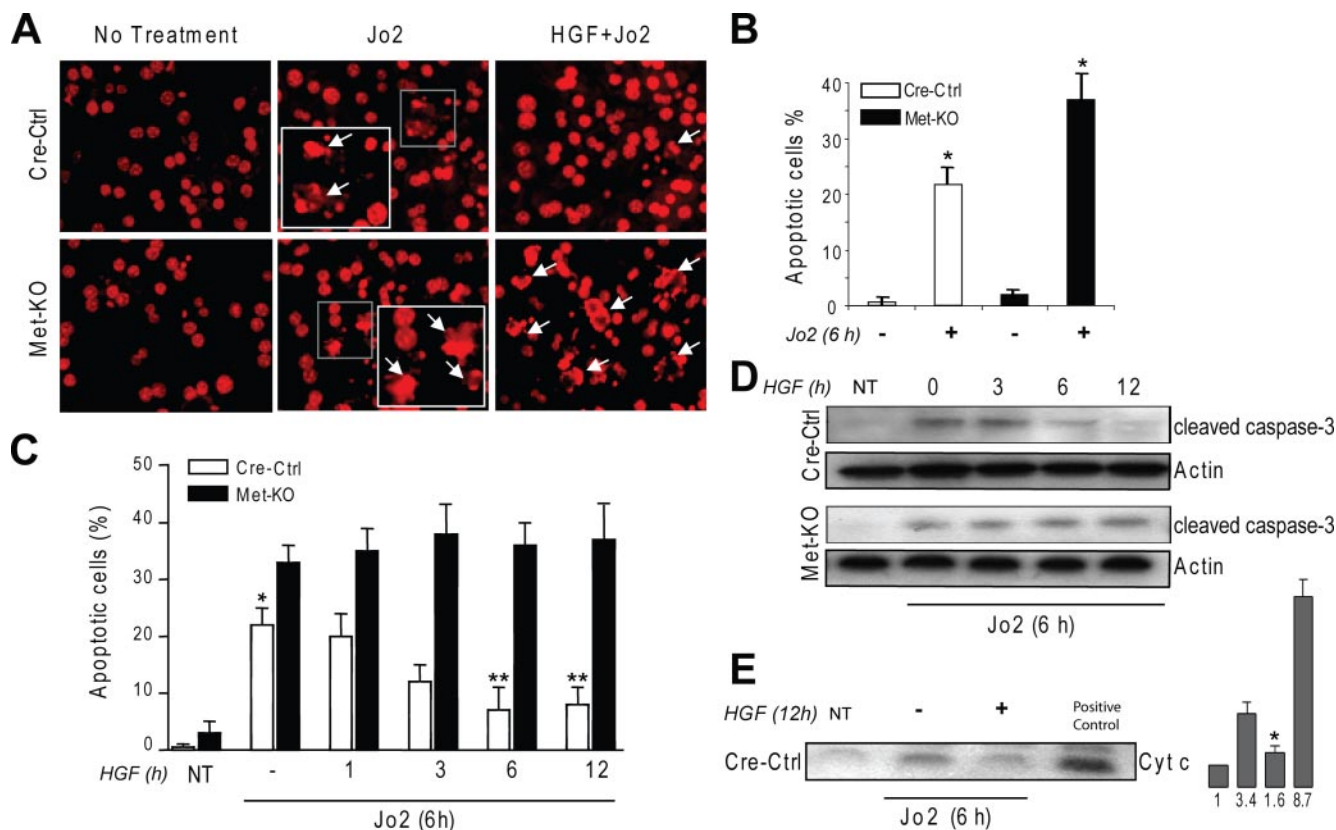
FIGURE 1. **Lack of c-Met function increases sensitivity of mouse hepatocytes to Jo2-mediated apoptosis.** *A,* representative images of primary hepatocytes stained with PI. Cre-Ctrl and Met-KO cultures were serum-starved for 16 h and incubated with Jo2 (0.5 μg/ml) for 6 h in the absence or presence of HGF (40 ng/ml) for 12 h. *Insets* show nuclear condensation, DNA fragmentation, and apoptotic body formation characteristic of apoptosis (*white arrowheads*). Original magnification, $\times$200. *B,* apoptotic index in Cre-Ctrl and Met-KO hepatocytes treated with Jo2 (0.5 μg/ml) for 6 h after serum starvation for 16 h. Each column represents the mean $\pm$ S.E. At least 500 nuclei were counted from duplicate cultures in three independent experiments. *, $p < 0.05$ against respective untreated cultures. *C,* time course of HGF protection against Jo2-induced apoptosis. Serum-starved (16 h) Cre-Ctrl and Met-KO hepatocytes were incubated with Jo2 (0.5 μg/ml) in the absence or presence of HGF (40 ng/ml) for the indicated time. Apoptotic index was detected by counting apoptotic cells after PI staining. Each column represents the mean $\pm$ S.E. At least 500 nuclei were counted from duplicate cultures in three independent experiments. *, $p < 0.05$ against respective Met-KO culture. **, $p < 0.05$ against Cre-Ctrl in the absence of HGF pretreatment. *NT,* no treatment. *D,* activation of caspase 3. Whole cell lysates from Cre-Ctrl and Met-KO hepatocytes were immunoblotted with anti-cleaved caspase-3. Treatment with HGF and Jo2 was performed as described in *C. E,* cytochrome *c* release. Cre-Ctrl hepatocytes were serum-starved for 16 h and incubated with Jo2 (0.5 μg/ml) for 6 h in the absence or presence of HGF (40 ng/ml) for 12 h. Cytosol fractions were immunoblotted with anti-cytochrome *c* (*Cyt c*). Mitochondrial protein was used as positive control. The intensity of each band was quantified by densitometry and expressed as fold of control (*NT*). A representative Western blot of three experiments is shown in *D* and *E.* *, $p < 0.05$ *versus* treated with Jo2.

GSH Determination by HPLC—GSH and GSSG content was determined by HPLC as described by Fariss and Reed (24) with some modifications. Briefly, cells were collected in 1 ml of 10% perchloric acid (Sigma), sonicated, and centrifuged at 5000 $\times$ *g* for 5 min at 4 °C. After removal of the supernatants, 100 mM iodoacetic acid (Sigma) in 0.2 mM *m*-cresol (Sigma) was added to each sample and GSH/GSSG solution standards, and the pH was adjusted to 9.0. Samples and standards were incubated in the dark for 1 h followed by the addition of 1 ml of 1% 1-fluoro-2,4-dinitrobenzene (Sigma) in 100% HPLC grade ethanol. *N*-Dinitrophenyl derivatives were injected (100 μl) into the loop of the HPLC system (Waters), and separated on a 3-aminopropyl column (5 μm; 4.6 mm $\times$ 20 cm; Custom LC, Houston, TX). Eluted *N*-dinitrophenyl derivatives were measured by ultraviolet detection at 365 nm.

Lipid Peroxidation Assay—Lipid peroxidation was assayed by the production of thiobarbituric acid-reactive components using spectrophotometry as described by Buege and Aust (25).

Analysis of NADPH Oxidase Activity—Untreated Cre-Ctrl and Met-KO cells were harvested, pelleted by centrifugation at

3000 $\times$ *g* for 5 min at 4 °C, and resuspended in PBS. NADPH oxidase was analyzed as described by Herrera *et al.* (26). Cells were incubated with 250 μM NADPH. NADPH consumption was monitored by the decrease in absorbance at $\lambda = 340$ nm for 5 min. Specific NADPH oxidase activity was determined by monitoring the rate of consumption of NADPH inhibited by 10 μM DPI that was added 30 min before the assay. An aliquot of cells lysed with SDS was used to determine protein content. Results were expressed as picomoles of oxidized NADPH per min per mg of protein.

Rac1 Activation Assay—The endogenous GTP-associated form of Rac1 was detected using Rac1 activation assay kit (Upstate Biotechnology, Inc.) according to the manufacturer's instructions. The same samples used for GTP-Rac1 precipitation were used to assay total Rac1 by Western blot using Rac1 monoclonal antibody.

Statistical Analysis—The data are presented as means $\pm$ S.E. for at least three independent experiments. Comparisons between groups were made using Student's *t* test. Differences were considered significant at $p < 0.05$.
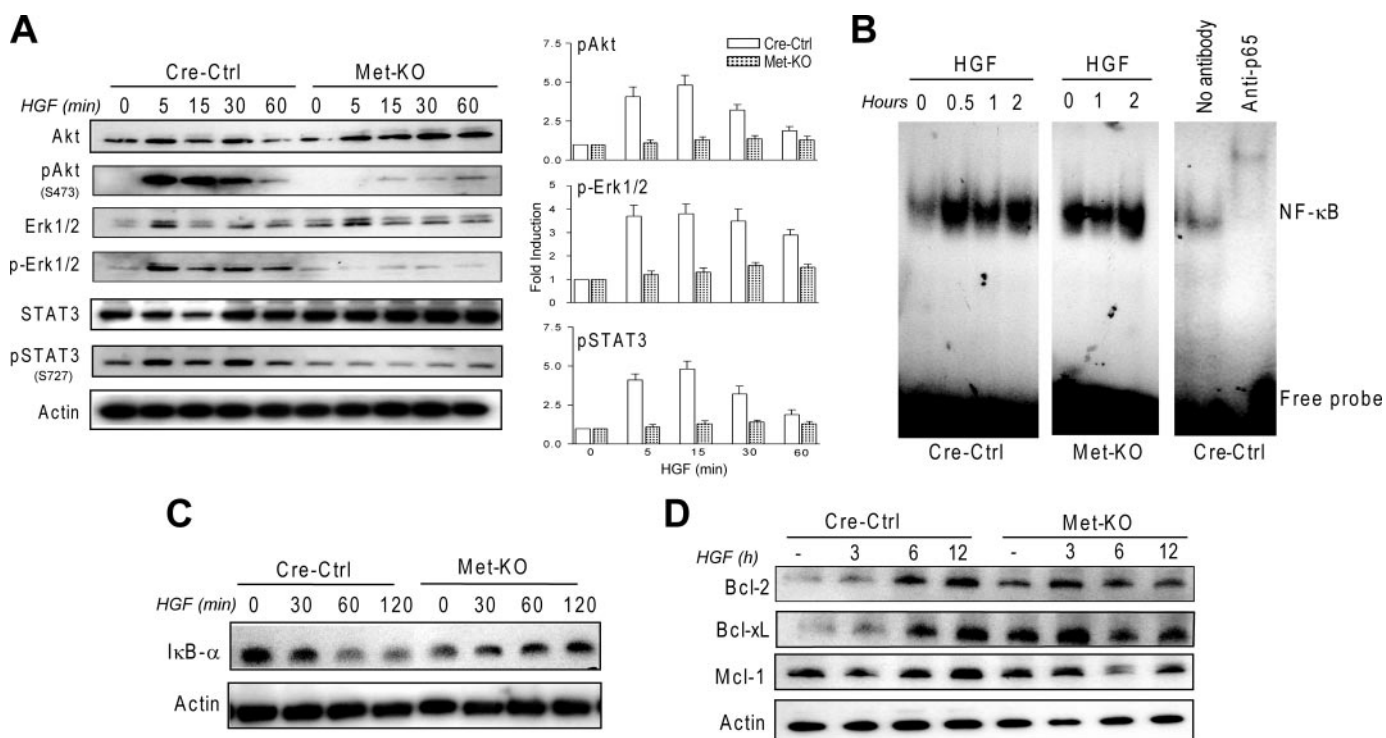
FIGURE 2. **Met-KO primary hepatocytes exhibit constitutive activation of NF-κB and antiapoptotic proteins.** *A,* HGF activates Akt, Erk1/2, and STAT3 in Cre-Ctrl but not Met-KO cells. Whole cell lysates prepared from serum-starved (16 h) Cre-Ctrl and Met-KO cultures treated with 40 ng/ml HGF for 0, 5, 15, 30, and 60 min were immunoblotted with anti-AKT, anti-Erk1/2, anti-Stat3, and phospho-specific antibodies against Akt Ser(P)-473, Erk1/2 Thr(P)-202/Tyr(P)-204, and Stat3 Ser(P)-727. The intensity of each protein was quantified by densitometry normalized to actin. The density value of total protein in untreated samples was designated as 1. Each *bar* represents the mean ± S.E. *B,* electromobility shift assay of NF-κB DNA binding activity in serum-starved (16 h) Cre-Ctrl and Met-KO hepatocytes treated with HGF (40 ng/ml) for the indicated time. The presence of supershift complex with anti-p65 demonstrates the assay specificity. *C,* kinetics of IκB degradation. Whole cell lysates prepared from serum-starved (16 h) Cre-Ctrl and Met-KO hepatocytes treated with 40 ng/ml HGF for 0, 30, 60, and 120 min were immunoblotted with anti-IκB-α. *D,* expression of antiapoptotic proteins in Cre-Ctrl and Met-KO cultures. Cre-Ctrl and Met-KO hepatocytes were serum-starved for 16 h and incubated with HGF (40 ng/ml) for the indicated time. Whole cell lysates were immunoblotted with anti-Bcl-2, anti-Bcl-xL, and anti-Mcl-1. A representative Western blot of three experiments is shown in *A, C,* and *D.*

RESULTS

Lack of c-Met Function Increases Sensitivity of Mouse Hepatocytes to Jo2-mediated Apoptosis—Consistent with our *in vivo* study (20), hepatocytes isolated from liver-specific c-Met conditional knock-out mice (Met-KO) were more susceptible to Jo2-mediated cell death as judged by apoptotic index (Fig. 1, *A* and *B*) and caspase 3 cleavage (not shown). As expected, HGF pretreatment provided no protection in Met-KO cultures but significantly inhibited cell death in Cre-Ctrl hepatocytes (Fig. 1*C*). The anti-apoptotic effect of HGF was time-dependent, peaked at 6 h of HGF exposure, and correlated with a decrease in caspase 3 activation and cytochrome *c* release (Fig. 1, *C–E*). These results provide genetic evidence for essential role of HGF/c-Met signaling in protecting mouse hepatocytes against Jo2-mediated apoptotic cell death.

PI3K/Akt Pathway Is Primarily Responsible for NF-κB Activation and Apoptosis Protection in Mouse Hepatocytes—To understand the molecular events underlying the increased rate of apoptosis in c-Met-deficient cells, we examined the activation of several survival pathways known to be involved in HGF-mediated cytoprotection (4). Phosphorylation of Akt, Erk1/2, and STAT3 was readily detectable in control hepatocytes within 5–60 min after HGF treatment and was abolished in Met-KO cultures (Fig. 2*A*).

Next, we determined which of these survival pathways played a major role in the protective effect of HGF in normal mouse hepatocytes. For this purpose, we used pharmacological and peptide inhibitors of PI3K, Erk1/2, and STAT3, and we assessed the activation of downstream transcription factor NF-κB by electrophoretic mobility shift assay. There is evidence that NF-κB protects mouse hepatocytes against Jo2-mediated apoptosis via subsequent induction of anti-apoptotic proteins (13, 27). In control cultures, HGF treatment rapidly increased NF-κB DNA binding activity that occurred in parallel with a time-dependent IκB-α degradation (Fig. 2, *B* and *C*). Maximum activity was achieved within 30 min and maintained for at least 2 h. In agreement with the biological response, HGF-induced activation of NF-κB was associated with up-regulation of the Bcl-2 family members. The protein levels of Bcl-2 and Bcl-xL were increased in whole cell lysates prepared from Cre-Ctrl hepatocytes after 3 h of HGF exposure and reached a maximum at 6–12 h (Fig. 2*D*). The expression of Mcl-1, which has been reported to be critical for the anti-apoptotic protection of human hepatocytes (13), was consistently high and increased to a lesser extent during the course of HGF treatment (Fig. 2*D*).

Inhibition of the PI3K pathway by either wortmannin or LY294002 completely abolished HGF-induced NF-κB binding activity, induction of Bcl-2 and Bcl-xL, and HGF-mediated protection against Jo2-induced apoptosis in Cre-Ctrl hepatocytes (Fig. 3, *A–C*). The protein levels of Mcl-1 were changed only modestly by these treatments (Fig. 3*B*). Conversely, in Met-KO cells that lacked HGF-mediated activation of the PI3K pathway
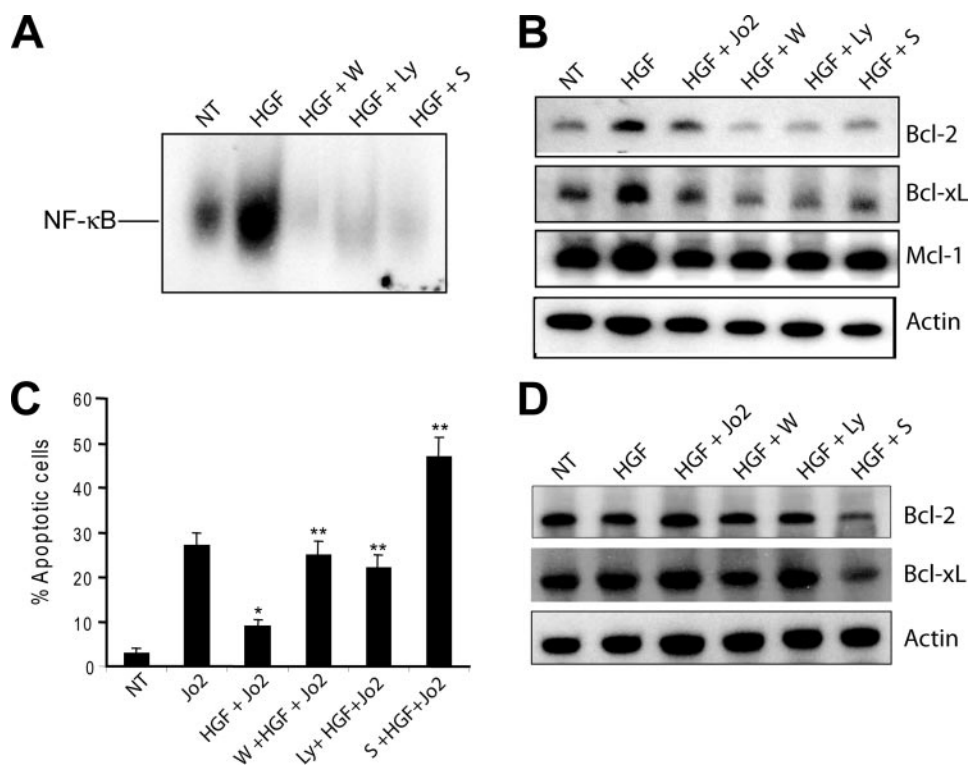
A

NF-κB ——

B

Bcl-2
Bcl-xL
Mcl-1
Actin

C

% Apoptotic cells

D

Bcl-2
Bcl-xL
Actin

FIGURE 3. **NF-κB activation is required for the antiapoptotic effects of HGF in Cre-Ctrl hepatocytes.** *A,* electromobility shift assays of NF-κB DNA binding activity. Cre-Ctrl hepatocytes were pretreated with 100 μM wortmannin (*W*), 50 μM LY294002 (*Ly*), and 100 μM sulfasalazine (*S*) for 30 min followed by 40 ng/ml HGF for 12 h. Results were confirmed in three independent experiments. *B,* expression of antiapoptotic proteins in Cre-Ctrl cells. Cells were pretreated with 100 μM wortmannin, 50 μM LY294002, and 100 μM sulfasalazine for 30 min followed by 40 ng/ml HGF for 12 h. *C,* effect of inhibition of PI3K/Akt and NF-κB on frequency of apoptosis. After 16 h of serum starvation, cells were pretreated with 100 μM wortmannin, 50 μM LY294002, or 100 μM sulfasalazine for 30 min followed by treatment with HGF (40 ng/ml) for 12 h and Jo2 (0.5 μg/ml) for the last 6 h in culture. Apoptotic index was detected by counting apoptotic cells after PI staining. Each column represents the mean ± S.E. At least 500 nuclei were counted from duplicate slides from three independent cultures. *D,* expression of antiapoptotic proteins in Met-KO cells. Cells were pretreated with 100 μM wortmannin, 50 μM LY294002, and 100 μM sulfasalazine for 30 min followed by 40 ng/ml HGF for 12 h. A representative Western blot of three experiments is shown in *B* and *D*. *, $p < 0.05$ against Jo2 treatment alone; **, $p < 0.05$ against HGF + Jo2 treatment. *NT,* no treatment.

mined whether the lack of c-Met function could have contributed to the intracellular redox changes. We found that ROS production was markedly stimulated by c-*met* deletion as judged by the peroxide-activated fluorescence dye DCFH-DA (Fig. 4*A*). In addition, the levels of malondialdehyde, a downstream measure of accumulated oxidative damage, were increased in c-Met-deficient hepatocytes, whereas the GSH/GSSG ratios were reduced as compared with the control cultures (Fig. 4, *B* and *C*). However, the proteins levels of the anti-oxidant enzymes catalase and superoxide dismutase were constitutively higher in c-Met knock-out cells, apparently as an adaptive response to compensate for the increased oxidative stress (Fig. 4*D*).

Increase in ROS production appeared to be regulated by the Nox-dependent mechanism given that ROS signal was blocked by known NADPH oxidase inhibitors such as diphenylene iodonium (DPI) and 4-(2-aminoethyl) benzenesulfonyl fluoride (Fig. 4*A*). Incubation with xanthine oxidase inhibitor (allopurinol) as well as with inducible nitric-oxide synthase (*N*-(3-(aminomethyl)benzyl)acetamidine) or Cox-2 (indomethacin) inhibitors did not block ROS generation attesting to the selectivity of the effect (Fig. 4*A*). The finding of DPI-sensitive increased ROS production in Met-KO cells was associated with a greater NADPH oxidase activity as well as up-regulation of Nox2 expression, a key component of the functional NADPH oxidase complex in hepatocytes (28–30) (Fig. 4, *E* and *F*). In line with these data, Met-KO primary hepatocytes also exhibited about a 2-fold increase in the biologically active form of Rac1 (GTP-bound Rac) (Fig. 4*G*) implicated in the assembly and activation of NADPH oxidase complex (31). In addition, c-Met-deficient hepatocytes displayed increased phosphorylation of several PKC isoforms (data not shown) reported to induce activating serine phosphorylation of p47*phox*, a regulatory subunit of the NADPH oxidase complex (29, 30). These results show that genetic inactivation of c-Met disrupts redox homeostasis in mouse hepatocytes because of the increased rate of NADPH-derived ROS generation.

GSH Synthesis Is Required for Apoptosis Protection—Given the prominent role of GSH in regulating redox balance in hepatocytes, we then tested the involvement of GSH in the sensitization of Met-KO cells to Jo2-mediated apoptosis. For this purpose, hepatocytes were cultured either in the presence of NAC, an antioxidant and GSH precursor, or BSO, an inhibitor of

(Fig. 2*A*), wortmannin and LY294002 did not affect expression of anti-apoptotic proteins (Fig. 3*D*), whereas treatment with the NF-κB inhibitor sulfasalazine was very effective in down-regulating Bcl-2 and Bcl-xL protein levels and inducing apoptosis in both cell types (Fig. 3, *B–D*, and Fig. 5*C*). Suppression of Erk1/2 and STAT3 signaling affected neither NF-κB activation nor cell survival (data not shown).

Met-KO Hepatocytes Exhibit Constitutive Activation of NF-κB—Interestingly, unchallenged c-Met-deficient hepatocytes exhibited greater NF-κB DNA binding activity in comparison with control cells regardless of HGF stimulation (Fig. 2*B*). Also, c-Met-deficient hepatocytes had higher basal levels of Bcl-2 and Bcl-xL, consistent with NF-κB electrophoretic mobility shift assay data, and comparable levels of Mcl-1. Nevertheless, abnormal activation of NF-κB and NF-κB-responsive genes was unable to protect c-Met-deficient hepatocytes against Jo2-induced apoptosis.

Met Deletion Increases Oxidative Stress—It is well known that NF-κB may be activated under oxidative stress conditions (16). Using microarray analysis, we have recently found dysregulation of genes involved in the oxidative stress response in c-Met-deficient primary hepatocytes (18). We therefore deter-
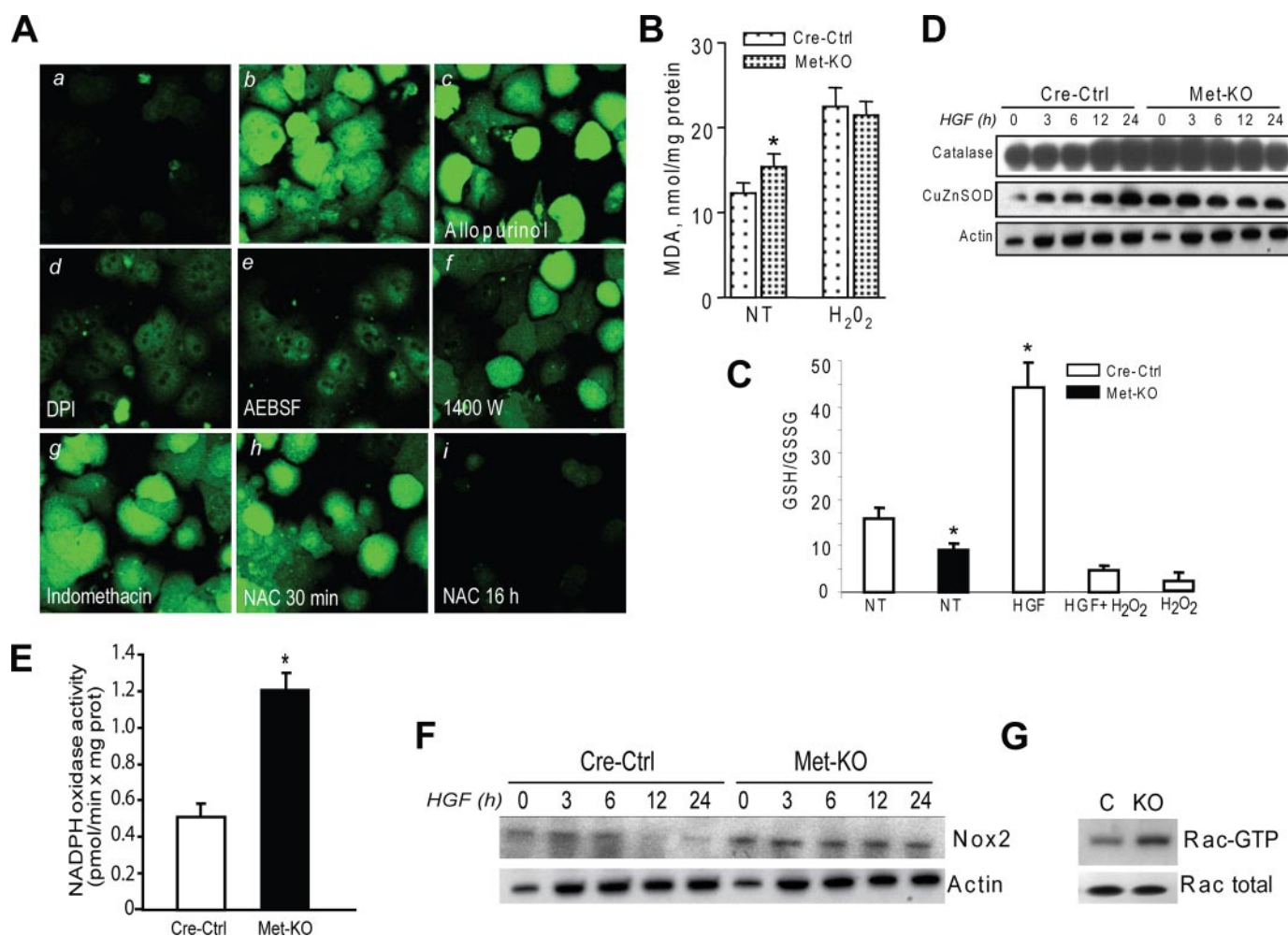
FIGURE 4. **Met-KO hepatocytes are subjected to oxidative stress.** *A,* Cre-Ctrl (*panel a*) and Met-KO (*panel b*) cells were incubated with the oxidative-sensitive probe DCFH-AM (3 μM) for 30 min. Met-KO cells were pretreated with 100 μM allopurinol (*panel c*), 100 μM DPI (*panel d*), 250 μM 4-(2-aminoethyl) benzenesulfonyl fluoride (*AEBSF*) (*panel e*), 100 μM *N*-(3-(aminomethyl)benzyl) acetamidine (*1400W*) (*panel f*), 100 μM indomethacin (*panel g*), and 10 mM NAC (*panel h*) for 30 min and 16 h (*panel i*) before incubation with 3 μM DCFH-AM for 30 min. Original magnification, $\times$100. *B,* lipid peroxidation was assessed by malondialdehyde (*MDA*) content in Cre-Ctrl and Met-KO hepatocytes after serum starvation for 16 h. Treatment with 0.25 mM H_2O_2 was used as positive control. Each *column* represents the mean $\pm$ S.E. of three independent experiments. *, $p < 0.05$ against Cre-Ctrl. *C,* ratio of reduced glutathione (GSH) to oxidized glutathione (GSSG) determined by HPLC in serum-starved Cre-Ctrl and Met-KO hepatocytes. Cre-Ctrl hepatocytes were treated with H_2O_2 (0.25 mM) for 6 h as positive control. Each column represents the mean $\pm$ S.E. of three independent experiments. *, $p < 0.05$ against untreated Cre-Ctrl. *NT,* no treatment. *D,* expression of antioxidant proteins. Whole cell lysates prepared from Cre-Ctrl and Met-KO hepatocytes treated with HGF (40 ng/ml) at 0, 3, 6, 12, and 24 h were immunoblotted with anti-catalase and anti-CuZn superoxide dismutase. A representative Western blot of three experiments is shown. *E,* NADPH oxidase activity. *F,* expression of Nox2. Whole cell lysates prepared and treated as described above (*D*) were immunoblotted with anti-Nox2. *G,* Rac1 activation assay. PAK-1 was used to pull down the activated Rac-GTP from Cre-Ctrl (*C*) and Met-KO (*KO*) cell lysates. Immunoblotting was performed using Rac1 monoclonal antibody to reveal the amount of total Rac1.

γ-glutamyl cysteine synthetase, the rate-limiting enzyme in the glutathione biosynthesis pathway. The results showed that NAC had a potent protective effect against Jo2-induced cell death. The number of Met-KO cells undergoing apoptosis was reduced 4-fold ($p < 0.05$) as compared with the cultures treated with Jo2 alone (Fig. 5*A*). Conversely, BSO completely abrogated both NAC- and HGF-mediated apoptosis protection in Met-KO cells and Cre-Ctrl cells, respectively (Fig. 5*A*), indicating a role for GSH in protection against Fas-induced apoptosis.

Persistent Activation of NF-κB Protects Met-KO Hepatocytes against ROS-related Toxicity—To further verify that NF-κB activation in Met-KO cells is because of increased oxidative stress, we incubated c-Met-deficient hepatocytes with the antioxidant NAC. Significantly, short term incubation with NAC

(30 min) failed to produce an immediate decrease in ROS levels (Fig. 4*A*). However, prolonged treatment with NAC (16 h) effectively blocked ROS generation and decreased the DNA binding activity of NF-κB to the levels found in untreated controls suggesting that *de novo* GSH synthesis may be responsible for reduced ROS generation (Fig. 4*A*).

Finally, we treated cells with a specific NF-κB peptide inhibitor SN50 that blocks NF-κB nuclear translocation. Exposure to SN50 significantly reduced survival of Met-KO hepatocytes concomitantly with a decrease in the DNA binding activity of NF-κB (Fig. 5, *B* and *C*). In contrast, inhibition of NF-κB in Cre-Ctrl cultures had small if any effect on cell viability (Fig. 5*C*). These results show that sustained NF-κB activation was sufficient to protect Met-KO hepatocytes against ROS-related toxicity under basal conditions.
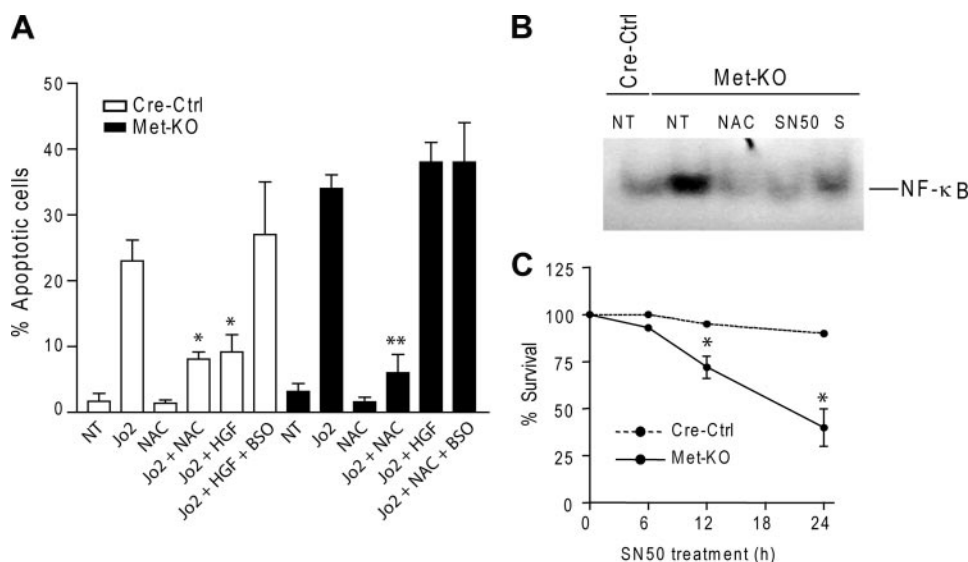
A

B

C

FIGURE 5. **Reduced GSH levels in Met-KO hepatocytes increase sensitivity to apoptosis.** *A,* Cre-Ctrl and Met-KO hepatocytes were pretreated with BSO (300 μM) for 1 h before incubation with HGF (40 ng/ml) or NAC (10 mM) for 12 h followed by Jo2 (0.5 μg/ml) treatment for 6 h. Apoptotic index was determined by counting apoptotic cells after propidium iodine staining. Each *column* represents the mean ± S.E. At least 500 nuclei were counted from duplicate cultures from three independent experiments. *, $p < 0.05$ against Cre-Ctrl cells treated with Jo2 alone or Jo2 + HGF + BSO; **, $p < 0.05$ against Met-KO treated with Jo2 alone, Jo2 + HGF, or Jo2 + NAC + BSO. *B,* electromobility shift assays of NF-κB DNA binding activity was performed using nuclear extracts from untreated (*NT*) Cre-Ctrl cells and Met-KO cells and Met-KO cells treated with 10 mM NAC, 30 μM SN50, or 100 μM sulfasalazine (*S*) for 12 h. *C,* cell viability in Cre-Ctrl and Met-KO hepatocytes treated with 30 μM SN50 for 24 h as determined by crystal violet assay. Mean ± S.E. of three independent experiments are shown. *, $p < 0.05$ against respective Cre-Ctrl cells.

DISCUSSION

In this study, we used both genetic and pharmacological approaches to address the molecular mechanisms of Met-triggered cell survival. As expected, primary hepatocytes established from liver-specific Met conditional knock-out mice failed to elicit the HGF-driven protection against apoptosis initiated by Jo2 treatment (Fig. 1). Similarly, blocking c-Met receptor with the specific c-Met inhibitor PHA-665752 abrogated the ability of protein-tyrosine phosphatase 1B knock-out hepatocytes to resist Fas-induced apoptosis, supporting a critical role for the functional Met in cytoprotection (32). Although the kinase activity of the Met receptor is essential for execution of the biological effects of HGF (33), a physical association between c-Met and Fas receptor has been recently found in c-Met overexpressing livers that blocked the interaction with Fas ligand, thus offering an alternative defense mechanism via suppression of Fas activation (34).

The survival program of HGF/c-Met signaling in adult and fetal hepatocytes is well established and includes primarily activation of PI3K/Akt as well as MAPK and STAT3 signaling pathways (12–14, 27, 34, 35). In agreement with these studies, we identified the PI3K/Akt pathway as a core element of HGF-triggered survival, which required NF-κB activation and subsequent induction of the Bcl-2 family apoptotic proteins such as Bcl-2 and Bcl-xL. Accordingly, pharmacological inhibition of PI3K/Akt pathway either by wortmannin or LY294002 completely abolished the HGF-induced NF-κB binding activity, up-regulation of Bcl-2 and Bcl-xL, as well as inhibition of Jo2-induced cell death. Although HGF stimulation also caused phosphorylation of MAPK and STAT3, blocking MAPK and

STAT3 with specific inhibitors affected neither NF-κB activation nor cell survival (Figs. 2 and 3).

HGF-triggered NF-κB activation correlated with up-regulation of Bcl-2 and Bcl-xL (36, 37), whereas levels of Mcl-1, another anti-apoptotic protein playing a prominent role in HGF cytoprotection of human hepatocytes (13), remained persistently high. Accumulation of Bcl-2 and Bcl-xL occurred in a time-dependent manner and peaked at 6 h after HGF treatment suggesting a requirement for *de novo* synthesis (Fig. 2). Previous studies have implicated NF-κB in HGF anti-apoptotic signaling (17, 27, 38), although in some cells HGF can block NF-κB activation as an anti-inflammatory response (39).

Intriguingly, knocking out Met rendered hepatocytes more sensitive to Jo2-initiated apoptosis despite the abnormal increase in the basal levels of NF-κB activation and concurrent up-regulation of downstream antiapoptotic proteins. It is well known that elevation in ROS and redox changes may result in NF-κB activation as a cytoprotective mechanism (40). When ROS levels exceed the physiological threshold, cell enters a state of oxidative stress, which can increase the sensitivity to apoptosis (11, 41, 42). Consistent with this, c-Met-deficient hepatocytes showed overproduction of ROS, elevated lipid peroxidation, and up-regulation of antioxidant proteins catalase and CuZn superoxide dismutase when cultured under basal conditions. In addition, the GSH/GSSG ratios were significantly decreased in Met-KO cells (Fig. 4). In the liver, GSH exists at millimolar concentrations and determines the cellular redox potential (43). Importantly, HGF can increase GSH levels by inducing γ-glutamylcysteine synthase, a key step enzyme in GSH synthesis (10). It has also been reported that NF-κB can directly regulate transcription of both subunits of γ-glutamylcysteine synthetase in the liver (44). Accordingly, we have found a 4-fold increase in GSH levels in Cre-Ctrl cells treated with HGF (Fig. 4).

To corroborate the importance of GSH in HGF/c-Met triggered inhibition of apoptosis, we used NAC, the *N*-acetyl derivative of the amino acid L-cysteine and a precursor in the formation of the GSH (45). NAC pretreatment significantly reduced Jo2-mediated cell death in Met-deficient cells. Conversely, the GSH-depleting agent BSO completely abrogated both NAC- and HGF-mediated apoptosis protection in Met-KO and Cre-Ctrl cells, respectively (Fig. 5). In addition, NAC effectively decreased the DNA binding activity of NF-κB in Met-KO cells to the levels found in Cre-Ctrl cells implicating oxidative stress in the persistent NF-κB activation. Furthermore, blocking NF-κB with a specific inhibitor SN50 significantly reduced sur-

vival of Met-KO hepatocytes, although it did not affect the viability in Cre-Ctrl cultures (Fig. 5). Together, the data suggest that persistent NF-κB signaling in Met-deficient cells was essential and sufficient to alleviate the adverse effects of ROS under basal conditions, but it could not provide the protection when challenged with increased oxidative load. In agreement with these data, we have recently found marked metabolic alterations and compensatory up-regulation of redox-sensitive transcription factor Nrf2 (nuclear factor (erythroid-derived 2)-like 2) and a broad regulator of ROS metabolism PGC-1α (peroxisome proliferator-activated receptor-γ coactivator 1α) under condition of prolonged abrogation of c-Met signaling (18, 19, 46).

NAC-dependent inhibition of apoptosis in Met-deficient cells supports the proposed antioxidant function of HGF. As reported in a series of recent papers, HGF protected against oxidative stress-related toxicity by enhancing ROS scavenging and/or suppressing ROS production in a variety of cell types (11, 15, 36). Consistent with these data, our results show that in primary mouse hepatocytes HGF exerts a dual effect by increasing the GSH pool and inhibiting the expression of Nox2, a key component of the functional NADPH oxidase complex in hepatocytes (Fig. 4) (28–30). The NADPH oxidase has been identified as a major source of ROS generation upon treatment with Fas ligand (29, 30). Furthermore, recent studies implicated Rac1, a member of a multimeric Nox complex, as a direct regulator of Nox-dependent ROS generation in nonphagocytic cells (31). Consistent with this interpretation, HGF has been reported to prevent ROS production via negative regulation of Rac1 in a hypoxia/reoxygenation model of oxidative stress and apoptosis (15). In line with this, Met-KO hepatocytes exhibited excessive ROS generation in parallel with elevated Rac1 and NADPH activities (Fig. 4). Although further studies are needed to investigate the upstream mechanisms that link c-Met and ROS, the findings suggest that activation of Nox2 and Rac1 is involved in the oxidative stress response triggered by c-Met deletion.

In conclusion, genetic inactivation of c-Met in mouse primary hepatocytes disrupts redox homeostasis that in turn initiates a series of adaptive cellular responses through modulation of NF-κB-dependent survival pathway. The findings provide a mechanistic explanation for the high susceptibility of c-Met-deleted cells to Fas-mediated apoptosis and present evidence that intact c-Met signaling is a critical factor in the protection against excessive generation of endogenous ROS.

REFERENCES

1. Peter, M. E., and Krammer, P. H. (2003) *Cell Death Differ.* **10,** 26–35
2. Ogasawara, J., Watanabe-Fukunaga, R., Adachi, M., Matsuzawa, A., Kasugai, T., Kitamura, Y., Itoh, N., Suda, T., and Nagata, S. (1993) *Nature* **364,** 806–809
3. Gao, C. F., and Vande Woude, G. F. (2005) *Cell Res.* **15,** 49–51
4. Comoglio, P. M. (2001) *Nat. Cell Biol.* **3,** E161–E162
5. Matsumoto, K., and Nakamura, T. (1996) *J. Biochem.* (*Tokyo*) **119,** 591–600
6. Uehara, Y., Minowa, O., Mori, C., Shiota, K., Kuno, J., Noda, T., and Kitamura, N. (1995) *Nature* **373,** 702–705
7. Schmidt, C., Bladt, F., Goedecke, S., Brinkmann, V., Zschiesche, W., Sharpe, M., Gherardi, E., and Birchmeier, C. (1995) *Nature* **373,** 699–702
8. Devadas, S., Hinshaw, J. A., Zaritskaya, L., and Williams, M. S. (2003) *Free Radic. Biol. Med.* **35,** 648–661
9. Ding, W. X., Ni, H. M., DiFrancesca, D., Stolz, D. B., and Yin, X. M. (2004) *Hepatology* **40,** 403–413
10. Tsuboi, S. (1999) *J. Biochem.* (*Tokyo*) **126,** 815–820
11. Kannan, R., Jin, M., Gamulescu, M.-A., and Hinton, D. (2004) *Free Radic. Biol. Med.* **37,** 166–175
12. Xiao, G. H., Jeffers, M., Bellacosa, A., Mitsuuchi, Y., Vande Woude, G. F., and Testa, J. R. (2001) *Proc. Natl. Acad. Sci. U. S. A.* **98,** 247–252
13. Schulze-Bergkamen, H., Brenner, D., Krueger, A., Suess, D., Fas, S. C., Frey, C. R., Dax, A., Zink, D., Buchler, P., Muller, M., and Krammer, P. H. (2004) *Hepatology* **39,** 645–654
14. Moumen, A., Ieraci, A., Patane, S., Sole, C., Comella, J. X., Dono, R., and Maina, F. (2007) *Hepatology* **45,** 1210–1217
15. Ozaki, M., Haga, S., Zhang, H. Q., Irani, K., and Suzuki, S. (2003) *Cell Death Differ.* **10,** 508–515
16. Gloire, G., Legrand-Poels, S., and Piette, J. (2006) *Biochem. Pharmacol.* **72,** 1493–1505
17. Fan, S., Gao, M., Meng, Q., Laterra, J. J., Symons, M. H., Coniglio, S., Pestell, R. G., Goldberg, I. D., and Rosen, E. M. (2005) *Oncogene* **24,** 1749–1766
18. Kaposi-Novak, P., Lee, J. S., Gomez-Quiroz, L., Coulouarn, C., Factor, V. M., and Thorgeirsson, S. S. (2006) *J. Clin. Investig.* **116,** 1582–1595
19. Takami, T., Kaposi-Novak, P., Uchida, K., Gomez-Quiroz, L. E., Conner, E. A., Factor, V. M., and Thorgeirsson, S. S. (2007) *Cancer Res.* **67,** 9844–9851
20. Huh, C.-G., Factor, V. M., Sanchez, A., Uchida, K., Conner, E. A., and Thorgeirsson, S. S. (2004) *Proc. Natl. Acad. Sci. U. S. A.* **101,** 4477–4482
21. Kao, C. Y., Factor, V. M., and Thorgeirsson, S. S. (1996) *Biochem. Biophys. Res. Commun.* **222,** 64–70
22. Sánchez, A., Factor, V. M., Espinoza, L. A., Schroeder, I. S., and Thorgeirsson, S. S. (2004) *Hepatology* **40,** 590–599
23. Nakagawa, T., Sawada, M., Gonzalez, F. J., Yokoi, T., and Kamataki, T. (1996) *Mutat. Res.* **360,** 181–186
24. Fariss, M. W., and Reed, D. J. (1987) *Methods Enzymol.* **143,** 101–109
25. Buege, J. A., and Aust, S. D. (1978) *Methods Enzymol.* **52,** 302–310
26. Herrera, B., Murillo, M. M., Alvarez-Barrientos, A., Beltran, J., Fernandez, M., and Fabregat, I. (2004) *Free Radic. Biol. Med.* **36,** 16–26
27. Hatano, E., and Brenner, D. A. (2001) *Am. J. Physiol.* **281,** G1357–G1368
28. Carmona-Cuenca, I., Herrera, B., Ventura, J. J., Roncero, C., Fernandez, M., and Fabregat, I. (2006) *J. Cell. Physiol.* **207,** 322–330
29. Reinehr, R., Becker, S., Eberle, A., Grether-Beck, S., and Haussinger, D. (2005) *J. Biol. Chem.* **280,** 27179–27194
30. Reinehr, R., Becker, S., Keitel, V., Eberle, A., Grether-Beck, S., and Haussinger, D. (2005) *Gastroenterology* **129,** 2009–2031
31. Cheng, G., Diebold, B. A., Hughes, Y., and Lambeth, J. D. (2006) *J. Biol. Chem.* **281,** 17718–17726
32. Arena, S., Pisacane, A., Mazzone, M., Comoglio, P. M., and Bardelli, A. (2007) *Proc. Natl. Acad. Sci. U. S. A.* **104,** 11412–11417
33. Wang, X., DeFrances, M. C., Dai, Y., Pediaditakis, P., Johnson, C., Bell, A., Michalopoulos, G. K., and Zarnegar, R. (2002) *Mol. Cell* **9,** 411–421
34. Sangwan, V., Paliouras, G. N., Cheng, A., Dube, N., Tremblay, M. L., and Park, M. (2006) *J. Biol. Chem.* **281,** 221–228
35. Haga, S., Terui, K., Zhang, H. Q., Enosawa, S., Ogawa, W., Inoue, H., Okuyama, T., Takeda, K., Akira, S., Ogino, T., Irani, K., and Ozaki, M. (2003) *J. Clin. Investig.* **112,** 989–998
36. Santangelo, C., Matarrese, P., Masella, R., Di Carlo, M. C., Di Lillo, A., Scazzocchio, B., Vecci, E., Malorni, W., Perfetti, R., and Anastasi, E. (2007) *J. Mol. Endocrinol.* **38,** 147–158
37. Fornoni, A., Li, H., Foschi, A., Striker, G. E., and Striker, L. J. (2001) *Am. J. Pathol.* **158,** 275–280

38. Muller, M., Morotti, A., and Ponzetto, C. (2002) *Mol. Cell. Biol.* **22,** 1060–1072
39. Min, J. K., Lee, Y. M., Kim, J. H., Kim, Y. M., Kim, S. W., Lee, S. Y., Gho, Y. S., Oh, G. T., and Kwon, Y. G. (2005) *Circ. Res.* **96,** 300–307
40. Dalton, T. P., Shertzer, H. G., and Puga, A. (1999) *Annu. Rev. Pharmacol. Toxicol.* **39,** 67–101
41. Tripathi, P., and Hildeman, D. (2004) *Apoptosis* **9,** 515–523
42. Shiba, D., and Shimamoto, N. (1999) *Free Radic. Biol. Med.* **27,** 1019–1026
43. Fernandez-Checa, J. C., and Kaplowitz, N. (2005) *Toxicol. Appl. Pharmacol.* **204,** 263–273
44. Morante, M., Sandoval, J., Gomez-Cabrera, M. C., Rodriguez, J. L., Pallardo, F. V., Viña, J. R., Torres, L., and Barber, T. (2005) *Free Radic. Res.* **39,** 1127–1138
45. Anderson, M. E., and Luo, J. L. (1998) *Semin. Liver Dis.* **18,** 415–424
46. St-Pierre, J., Drori, S., Uldry, M., Silvaggi, J. M., Rhee, J., Jager, S., Handschin, C., Zheng, K., Lin, J., Yang, W., Simon, D. K., Bachoo, R., and Spirgelman, B. M. (2006) *Cell* **127,** 397–408